

## B-2.3 Estimation of methane emissions from the West Siberian Lowland by use of remote sensing and modeling techniques

**Contact person** : TAMURA Masayuki

Information processing and Analysis section  
Social and Environmental Systems Division  
National Institute for Environmental Studies, Japan Environment Agency  
16-2 Onogawa, Tsukuba, Ibaraki, Japan, 305-0053  
Tel: +81-298-50.2479, Fax: +81-298-50-2572,  
E-mail: m-tamura@nies.go.jp

**Total Budget for FY 1997-FY1999**: 37,174,000 Yen (FY1999: 12,044,000 Yen)

**Abstract** A method is presented for differentiating wetland areas in northern high-latitude zones using Normalized Difference Vegetation Index (NDVI) and land surface temperature ( $T_s$ ) calculated from midday NOAA/AVHRR imagery. Wetland areas have been distinguished from other land-cover types using signatures on a scattergram of NDVI vs.  $T_s$ . The method was applied for differentiating wetland areas in the basin of the Ob River in the west Siberian lowland. The result has been verified with ground-truth data and land-cover classification results obtained from high-resolution satellite images.

**Key Words**: NOAA/AVHRR, vegetation index, surface temperature, SPOT/HRV, wetland

### 1. Introduction

The west Siberian lowland is presumed to be a large source of atmospheric methane, which is the second most important greenhouse gas after carbon dioxide. The Japan-Russia joint research project conducted since 1991 by the National Institute for Environmental Studies (NIES) and Russian researchers has produced results confirming this presumption<sup>1</sup>. As basic data for estimating regional-scale methane fluxes from the west Siberian lowland, it is necessary to measure the distribution and areal extent of wetlands and to monitor seasonal changes of vegetation and surface conditions such as surface temperature and water level. Since detailed geographic information is not available in west Siberia and it is often difficult to access wetlands by ground vehicles, satellite or aerial images are necessary for investigating wetland ecosystems and mapping the geographic distribution of wetlands. In this study we present a method for differentiating wetland areas in west Siberia using midday NOAA/AVHRR imagery. Use of AVHRR data makes it possible to map the geographic distribution of wetlands with 1 km ground resolution.

### 2. Study area

Fig. 1 (a) shows the AVHRR image taken at 7:21 GMT (around 13:00 in local solar time) on 8th July 1995 in the basin of the Ob River. It covers a rectangular area centered at (82°E, 58°N) with a width 450 km and a height 415 km. The Ob River flows from bottom right to top left. Wetlands and forests occupies most part of the image area, and there are also several villages and agricultural lands along rivers. The bright spots near the bottom right corner show the city of Tomsk. The wetlands are mainly covered with sphagnum mosses, sedges, cotton grasses, reeds,

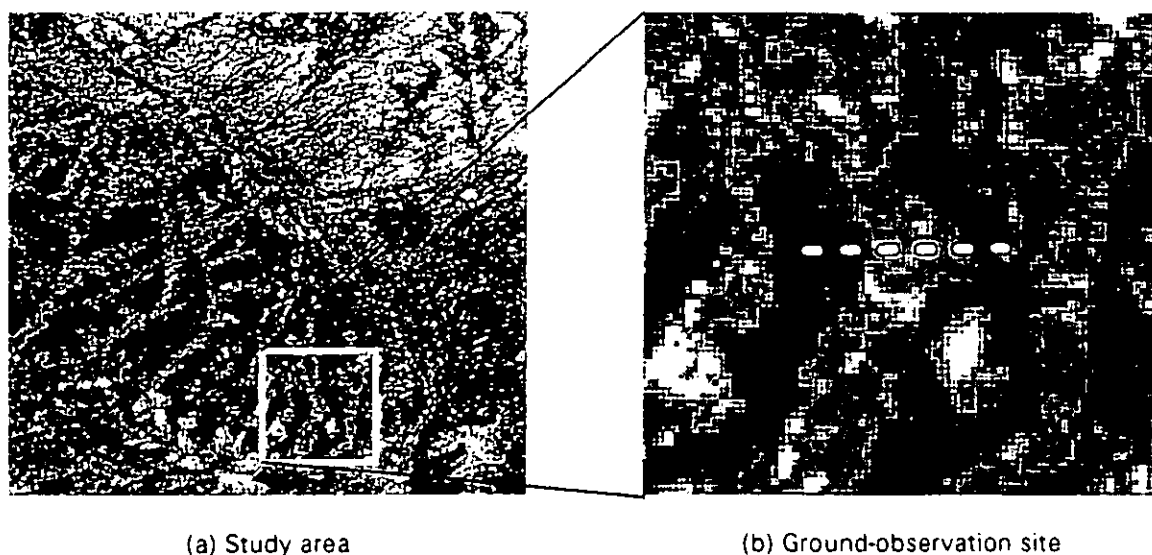


Fig. 1. (a) AVHRR image (in Band 1) obtained on 8th July 1995 in the Ob Basin. Area size: 450 km wide and 415 km long. Scene center: (82°E, 58°N). (b) Ground-observation site.

dwarf shrubs and low pine trees. The forest vegetation consists of both deciduous trees (birches and aspens) and coniferous trees (pines and larches).

The image includes the mires where the NIES and Russian researches are making ground observations of wetland vegetation, methane fluxes, surface temperatures and water levels. The location of the ground-observation site is indicated by the white rectangle in Fig. 1 (a), and its enlarged image is shown in Fig. 1 (b).

### 3. Differentiation of wetland areas

#### 3.1 Spatial profiles of AVHRR data

Fig. 2 shows the spatial profiles of AVHRR data along the transect line (white dotted line) indicated in Fig. 1 (b). The abscissa denotes distance in a pixel unit; the ordinate denotes reflectance (%) for visible and near infrared bands (bands 1 and 2), and radiometric brightness temperature (°C) for thermal bands (bands 3-5). The interval between 6 to 22 pixel distance corresponds to a wetland area; the rest parts correspond to forest areas. We see that from the spatial profile characteristics, AVHRR spectral band data can be classified into three groups, i.e. band 1, band 2, and bands 3-5. Band 1 reflectance is higher in wetlands than in forests. It can be explained by the fact that majority of sphagnum mosses found in this region take on brownish color, having higher reflectance in red band than forest green leaves. Band 2 data have higher values in forests than in wetlands, which demonstrates that green leaves have higher reflectance than sphagnum mosses in near infrared band. The dip from 18 to 21 pixel distance correspond to the place where wetlands have been dried by digging trenches. The bands 3-5 have more or less the same spatial profiles, having higher brightness temperatures in wetlands than in forests. This temperature difference may be explained by two mechanisms. First, forests may have a greater transpiration rate than wetlands; thus, forests have lower surface temperature in midday due to greater latent heat transfer. Second, forest leaves may be cooled by air until leaf temperatures are

in close adjustment with air temperatures<sup>2</sup>; on the other hand wetland plants represented by sphagnum mosses may be less cooled by air because they grow in dense clusters near or at the ground surface. We note that surface temperatures have highest values in dried parts of wetlands.

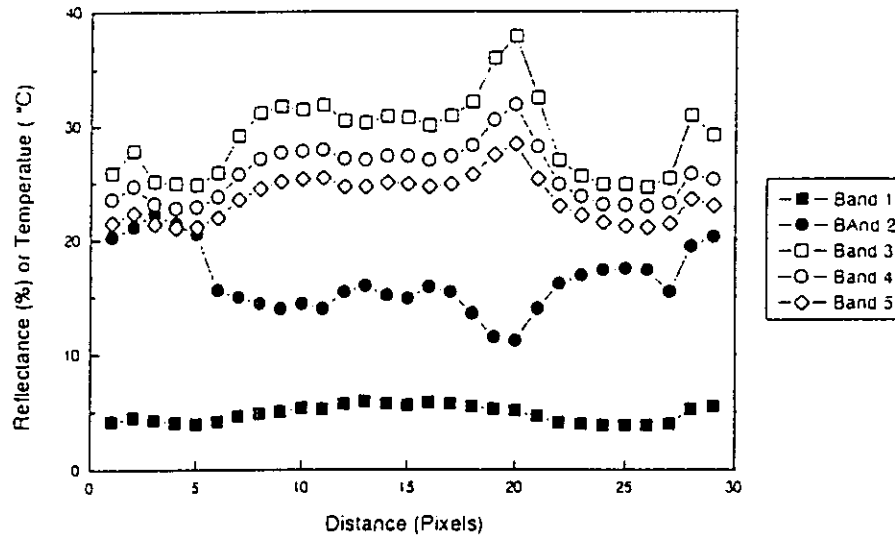


Fig. 2. Spatial profiles of AVHRR data along the transect line in Fig. 1 (b).

From the observation of the spatial profiles of AVHRR data, we have chosen two indices for delineating land cover types in the study area. One is the Normalized Difference Vegetation Index (NDVI) :

$$NDVI = \frac{NIR - RED}{NIR + RED}$$

where RED and NIR are reflectance values of bands 1 and 2 of the AVHRR. The other is surface temperature ( $T_s$ ) computed by the split-window method<sup>3</sup>:

$$T_s = 1.764 T_4 - 0.764 T_5 + 0.78$$

where  $T_4$  and  $T_5$  are radiometric brightness temperatures derived from AVHRR bands 4 and 5 respectively. Fig. 3 shows the spatial profiles of NDVI and  $T_s$  along the same transect line as in Fig. 2. We can see there is a negative correlation between NDVI and  $T_s$ , which has been observed by several researchers for various types of ecosystems<sup>4,5,6,7</sup>. NDVI expresses spectral reflectance properties and density of vegetation; surface temperature, on the other hand, is related to water and energy balance determined by moisture availability, amount of evapotranspiration and local climate factors. Since wetland vegetation has different features from other land-cover types in vegetation properties and moisture status, we can expect that wetland areas can be differentiated from other land-cover types by using NDVI and surface temperature as feature-extraction axes.

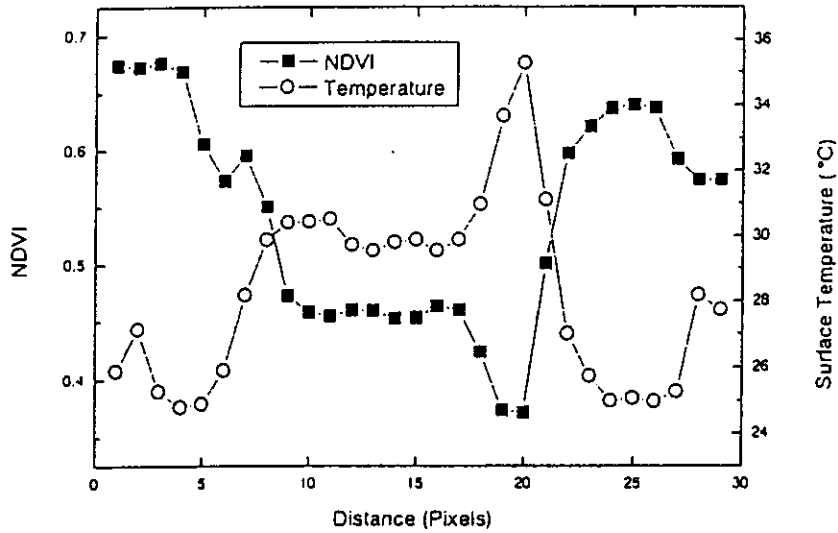


Fig. 3. Spatial profiles of NDVI and surface temperature along the transect line in Fig. 1 (b).

### 3.2 Land-cover classification by NDVI and surface temperature

Figs. 4 (a) and (b) illustrate NDVI and surface temperature for the study area respectively. The relation between NDVI and surface temperature can be visualized by a two-dimensional scattergram of NDVI vs.  $T_s$ . (Fig. 5). The location of each pixel on the scattergram is determined by the status of vegetation cover and moisture availability. We can hence expect that ecosystems having different properties in vegetation cover and moisture conditions occupy different places on the scattergram.



(a) NDVI



(b) Surface temperature

Fig. 4. Study area seen in (a) NDVI and (b) surface temperature.

Signatures of eight land-cover types typically found in this region were drawn on the scattergram: wetlands, birch forests, conifer forests, grasses, soils, rivers, lakes and clouds. The rectangles and '+' signs in Fig. 5 indicate the boundaries and means of training samples of the signatures. Signatures of birch forests, conifer forests, wetlands and soils are placed along a line of a negative slope in descending order of NDVI and in ascending order of  $T_s$ . The signature of grasses is located above this line, having higher surface temperatures than wetlands and forests. Lakes and rivers have almost the same surface temperature, but have different NDVI values due to the turbidity of river water. We note that existence of water surface in a pixel tend to shift the location of its scatterplot toward the signature of lake or river water. Clouds are characterized by their low surface temperatures and relatively low NDVI values. Pixels partly contaminated by clouds are shifted toward the signature of clouds.

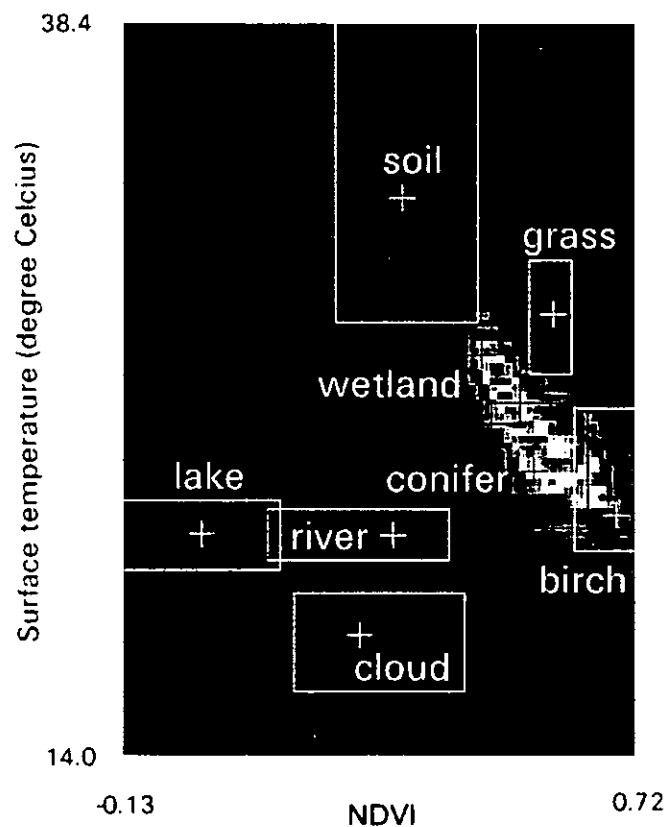


Fig. 5. Scattergram of NDVI vs.  $T_s$ . The rectangles and '+' signs show the boundaries and means of signatures.

Using these signatures we classified land-cover types by combined use of parallelepiped decision rule and minimum-distance decision rule. Fig. 6 shows the result of classification. From this result wetlands were estimated to cover 29 % of the entire image area, and forests cover 67 %. For verification, this result was compared with results of land-cover classification obtained from high-resolution satellite images (SPOT/HRV and JERS-1/OPS). For example Fig. 7 (a) shows the result of land-cover classification by SPOT/HRV. Fig. 7 (b) shows the area in Fig. 6 corresponding to the SPOT/HRV image. In both figures wetland areas are indicated by white colors. We can say both results are in fairly good agreement.

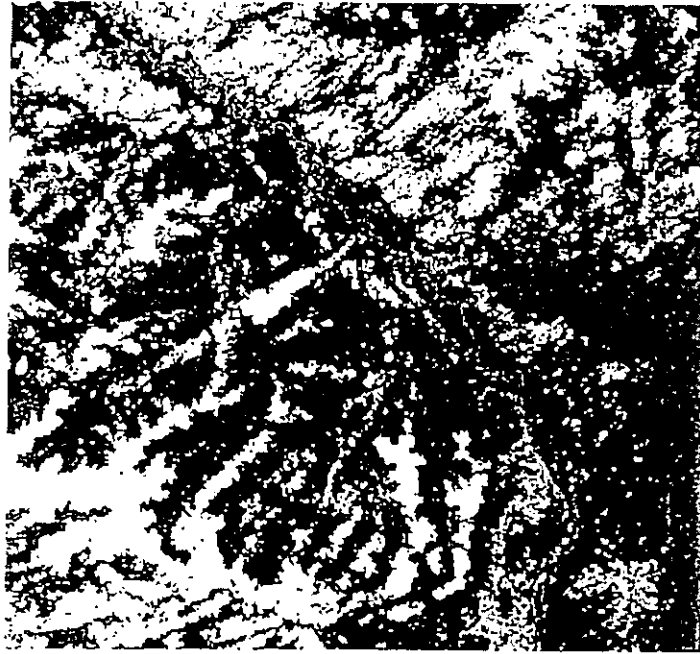
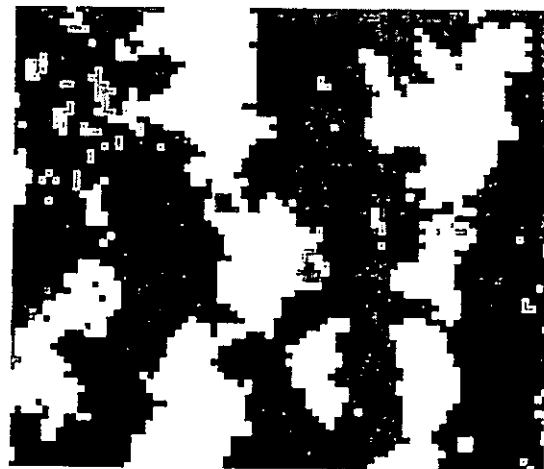


Fig. 6. Result of land-cover classification using NDVI and surface temperature.



(a) SPOT/HRV



(b) NOAA/AVHRR

Fig. 7. Comparison with the result of land-cover classification obtained from a high-resolution satellite image. (a) Result from SPOT/HRV. (b) Result from NOAA/AVHRR.

#### 4. Summary

Two indices calculated from midday NOAA/AVHRR data (NDVI and surface temperature  $T_s$ ) have been used to differentiate wetland areas in the basin of Ob River in the west Siberian lowland. From the observation of the spatial profiles of AVHRR data, we have chosen NDVI and  $T_s$  to be suitable for differentiating wetlands from other land-cover types. NDVI reflects properties of vegetation cover. Surface temperature is related to surface energy balance determined by moisture availability and evapotranspiration. A scattergram of NDVI vs.  $T_s$  has shown a negative correlation between these indices. NDVI is high in forests and low in wetlands, whereas surface temperature is low in forests and high in wetlands. Signatures of eight typical land-covers (wetlands, birch forests, conifer forests, grasslands, soils, lakes, rivers and clouds) have been drawn on the scattergram of NDVI vs.  $T_s$ . Based on these signatures wetland areas have been distinguished from other land cover types by combined use of parallelepiped decision rule and minimum-distance decision rule. The results have been verified by ground-truth data and by comparison with the results of land-cover classification obtained from high-resolution satellite images.

#### 5. References

1. N. S. Panikov, "CH<sub>4</sub> and CO<sub>2</sub> emission from northern wetlands of Russia," Proceedings of the International Symposium on Global Cycles of Atmospheric Greenhouse Gases, pp. 100-112, 1994.
2. D. M. Gate, *Biophysical Ecology*, Springer-Verlag, New York, 1980.
3. S. M. Singh, "Removal of atmospheric effects on a pixel by pixel basis from the thermal infrared data from instruments on satellites," *Int. J. Remote Sensing*, vol. 5, pp. 161-183, 1984.
4. J. C. Price, "Using spatial context in satellite data to infer regional scale evapotranspiration," *IEEE Trans. Geosci. Remote Sensing*, vol. 28, pp. 940-948, 1990.
5. R. Nemani, L. Pierce, and S. Running, "Developing satellite-derived estimates of surface moisture status," *J. Appl. Meteor.*, vol. 32, pp. 548-557, 1993.
6. M. A. Friedl and F. W. Davis, "Sources of variation in radiometric surface temperature over a tallgrass prairie," *Remote Sens. Environ.*, vol 48, pp. 1-17, 1994.
7. E. F. Lambin and D. Ehrlich, "The surface temperature-vegetation index space for land cover and land-cover change analysis," *Int. J. Remote Sensing*, vol. 17, pp. 463-487, 1996.